Intrinsically Disordered Proteins

DOI: 10.1002/anie.201308389

Compensatory Adaptations of Structural Dynamics in an Intrinsically Disordered Protein Complex**

Dennis Kurzbach, Thomas C. Schwarz, Gerald Platzer, Simone Höfler, Dariush Hinderberger, and Robert Konrat**

Abstract: *Intrinsically disordered proteins (IDPs) play crucial roles in protein interaction networks and in this context frequently constitute important hubs and interfaces. Here we show by a combination of NMR and EPR spectroscopy that the binding of the cytokine osteopontin (OPN) to its natural ligand, heparin, is accompanied by thermodynamically compensating structural adaptations. The core segment of OPN expands upon binding. This "unfolding-upon-binding" is governed primarily through electrostatic interactions between heparin and charged patches along the protein backbone and compensates for entropic penalties due to heparin–OPN binding. It is shown how structural unfolding compensates for entropic losses through ligand binding in IDPs and elucidates the interplay between structure and thermodynamics of rapid substrate-binding and -release events in IDP interaction networks.*

Intrinsically disordered proteins (IDPs) fulfill essential tasks in eukaryotic life despite a lack of well-defined structure. In particular, many IDPs are associated with versatile functions in protein interaction networks.[1] It is their structural flexibility that allows them to adapt to and to interact with different binding partners, making IDPs suited for functioning as hubs between several interaction partners.[2] However, this dynamic nature makes IDPs difficult to analyze. NMR spectroscopy has matured to a powerful experimental method for the characterization of IDPs and their complexes in solution.[3] The binding modes between IDPs and their ligands nonetheless remain vaguely described. Different mechanisms have been distinguished: among them so-called "folding-upon-binding",[4] where the IDP adopts a certain conformation when interacting with a ligand, and the formation of "fuzzy" complexes, where the IDP samples many conformations on the surface of a binding partner.[5] Since IDPs are typically more highly charged than globular proteins, electrostatics play a pronounced role in mediating the protein–ligand interactions of an IDP.[6] Specific charge patterns of IDPs have been found to be optimized for attraction to and interaction with their naturally charged substrates.[7] Here we provide, by a combination of NMR and electron paramagnetic resonance (EPR) data, unprecedented insight into the subtleties of conformational adaptations occurring in IDP–substrate recognition events. While NMR measurements provide residue-resolved information about structure (PRE; paramagnetic relaxation enhancement) and dynamics (NMR spin relaxation), EPR yields coarse-grained information about large-scale structural adaptations of IDPs.[8] We analyze the interaction of the IDP osteopontin (OPN), an extracellular matrix protein associated with metastasis of several kinds of cancer,[9] with heparin,[8f] a highly sulfated glycosaminoglycan widely used as an anticoagulant. In a biological context heparin binding to OPN is of interest since it models the OPN–heparan sulfate and/or hyaluronic acid interaction, which is assumed to be involved in the OPN-CD44 receptor (a heparan sulfate proteoglycan (HSPG) that sequesters various heparin-binding growth factors and chemokines) association—a process involved in cell signaling and adhesion.[9b] Glycosaminoglycans like heparin, hyalorunan, and heparan sulfate are crucial for chemokine function in vivo.[9c,d] Additionally, interactions between IDPs and biological polyelectrolytes are quite common[1b] and our results might well be applicable to other systems. We show that upon binding to heparin, OPN largely remains disordered although its structural ensemble is updated. The compensatory adaptations observed for OPN as a consequence of the heparin binding are mediated predominantly through electrostatic interactions and intriguingly demonstrate how entropic penalties due to the local rigidification of binding site residues upon ligand binding are compensated through the partial unfolding of peptide segments remote to the primary binding site. These results are important in the sense that they help to interpret the so far not well understood interplay between structure and thermodynamics of rapid substrate-binding and -release events in IDP interaction networks.

We investigate a 220 residue long mutant of OPN (amino acids 45–264 of native OPN plus an N-terminal Met). In Figure 1a) PRE changes upon heparin binding, ΔPRE, for

[*] Dr. D. Kurzbach,[+] T. C. Schwarz,[+] G. Platzer, S. Höfler, Prof. R. Konrat
Department of Structural and Computational Biology
Max F. Perutz Laboratories
Vienna Biocenter Campus 5, 1030 Vienna (Austria)
E-mail: robert.konrat@univie.ac.at
Prof. D. Hinderberger
Institute of Chemistry, Physical Chemistry (Complex Self-Organizing Systems)
Martin-Luther-University Halle-Wittenberg
Von-Danckelmann-Platz 4, 06120 Halle (Saale) (Germany)
E-mail: dariush.hinderberger@chemie.uni-halle.de
[+] These authors contributed equally to this work.

[**] We thank Christian Bauer for technical support and Prof. Hans W. Spiess for continuing support. D.K. acknowledges a Feodor-Lynen Scholarship from the Humboldt Foundation and support by the Gutenberg Academy of the University of Mainz. This work was supported by FWF (W-1221-B03). The expression plasmid for wild-type OPN was provided by the group of Prof. K. Bister (University of Innsbruck).

Supporting information for this article is available on the WWW under http://dx.doi.org/10.1002/anie.201308389.

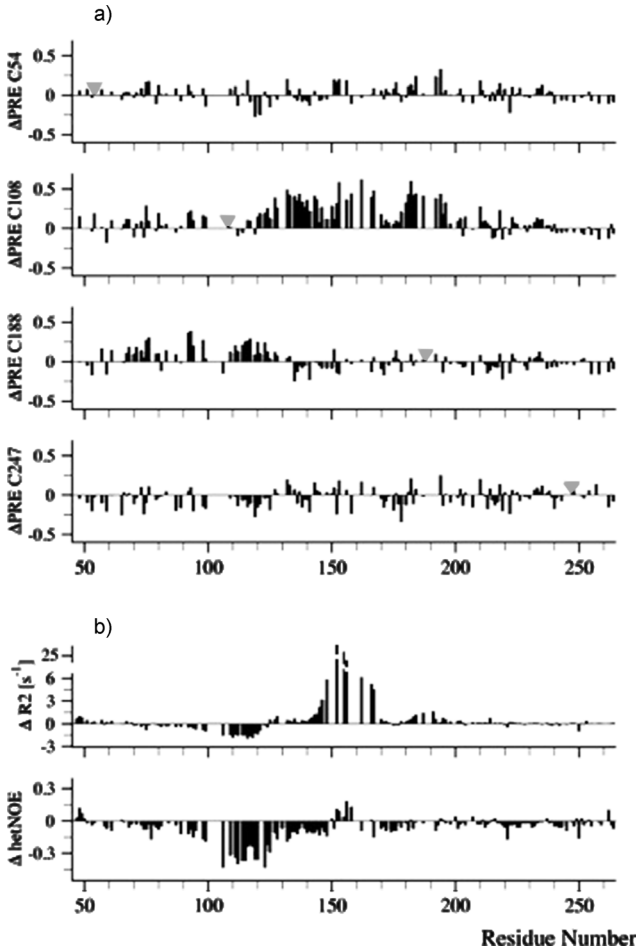

Figure 1. a) ΔPRE values for the four different labeling sites upon heparin binding derived from changes in ^{15}N-^{1}H HSQC signal intensities. (ΔPRE value is the relative (OPN-MTSL/OPN) ^{15}N-^{1}H HSQC intensity (heparin-bound) minus the relative ^{15}N-^{1}H HSQC intensity (apo)). ΔPRE values >0 indicate increasing distances to the labeling site (gray triangles mark the spin-labeled sites); ΔPRE values <0 indicate decreasing distances. For error estimates see the Supporting Information. b) ΔR_2 and ΔHetNOE (^{15}N-^{1}H NOE changes (bound minus apo)) as a function of residue position. For error estimates see the Supporting Information.

four spin-labeled Cys mutants of the truncated IDP are shown (labeling with MTSL; *S*-(2,2,5,5-tetramethyl-2,5-dihydro-^{1}H-pyrrol-3-yl)methyl methanesulfonothioate, mutants C54, C108, C188, and C247). ΔPRE values are calculated through changes in the relative (labeled/wildtype) ^{15}N-^{1}H HSQC signal intensity ratios (height) upon heparin binding of OPN (MTSL protein interactions were excluded by reference measurements; see the Supporting Information). When interpreting PRE values of IDPs one should be aware that due to the rapid conformational sampling of IDPs one observes ensemble-averaged PRE data.[8a] Hence, all conclusions drawn from these refer to "average" conformations and $\Delta PRE > 0$ indicates "on average" increasing distance between a labeling site and a residue upon binding, $\Delta PRE < 0$ the opposite.[8f] As can be observed, the IDP displays differential changes of long-range backbone interactions as heparin binds. Specifically, spin labels attached to residues C108 and C188 experience displacements from the core region, that is, from residues 120–200 for C108 and from 70–120 for C188. Concluding, the PRE data indicate that the central segment (residues 90–150) of OPN expands upon heparin binding, comparable to an "unfolding-upon-binding" event. Intermolecular PRE contributions have been ruled out by a control experiment using a mixture of ^{14}N-labeled MTSL-tagged and ^{15}N-labeled untagged OPN (see the Supporting Information).

Differential changes in the structural compactness of the central region of OPN are further reflected in its motional dynamics. These were monitored by ^{15}N relaxation measurements (^{15}N longitudinal relaxation rates R_1 and transverse relaxation rates R_2 and ^{15}N-^{1}H heteronuclear Overhauser enhancement, NOE) both in the apo (ligand-free) and heparin-bound state. Figure 1b shows a residue plot of ^{15}N R_2 and ^{15}N-^{1}H heteronuclear NOE differences. The regions containing most of the heparin binding site (residues 140–170 and 180–200) display an increase in ^{15}N R_2 values due to local rigidification of the backbone upon binding (motions on the nanosecond timescale). This is paralleled by larger ^{15}N-^{1}H heteronuclear NOE values (Figure 1b bottom) indicating reduced fast backbone motions on the picosecond timescale. In contrast, the region encompassing residues 90–120 exhibits increased backbone flexibility as evidenced by both decreased R_2 values and more negative heteronuclear NOEs. The finding that residues 90–120 are more flexible in the heparin-bound state is in good agreement with decreased PRE values and further validates that this part of the protein becomes more displaced from the heparin binding site and thus less restrained upon complex formation. Overall, the NMR relaxation data demonstrates that OPN displays more conformational flexibility in the bound state. The binding of heparin was further confirmed by DOSY (diffusion ordered spectroscopy) NMR measurements, which showed an increase of the hydrodynamic radius of OPN through heparin binding from 3.6 nm to 5.2 nm.

To complement the NMR-derived data on OPN we performed both room-temperature continuous-wave (CW) EPR measurements on the four available single mutants and double electron–electron resonance (DEER) measurements on six spin-labeled Cys double mutants of the truncation mutant. (DEER was performed at 50 K on shock-frozen samples that contain the conformational protein ensemble present at the glass-transition temperature of the solution, which is assumed to be representative for the solution structural ensemble. For further details see the Supporting Information.) CW EPR reveals that the label attached to residue C108 gains mobility through heparin binding, while the mutant C188 exhibits a more restricted rotational motion (with rotational correlations times of $\tau_{c,108} = 0.52$ ns, $\tau_{c,108/Heparin} = 0.43$ ns, $\tau_{c,188} = 0.69$ ns, and $\tau_{c,188/Heparin} = 0.87$ ns; see the Supporting Information). τ_c values of spin labels attached to residues C54 and C247 appear not to be affected significantly by heparin binding. Again, the increasing rotational mobility of MTSL at C108 is indicative of the pronounced solvent exposure of this labeling site as a consequence of the expansion of the core segment of OPN.[10] Note that τ_c values derived from CW EPR suffer from the nonseparability of local and global rotational correlation times (similar to

NMR data) and only represent an effective correlation time corresponding to the nitroxide moiety motion. To unequivocally probe changes of rotational correlation times due to binding of the ligand both NMR (R_2 and HetNOE) and EPR data are required.

While detailed characterization and analysis of the DEER time traces of the OPN apo state have already been reported,[11] here the DEER data were recorded in the absence and the presence of heparin. All DEER data are shown in the Supporting Information. As described previously, DEER data of IDPs with broad conformational ensembles are difficult to analyze due to a lack of signal modulation.[8d,11] Thus, since the standard DEER analysis techniques fail for OPN, time traces were analyzed using an effective modulation depth, Δ_{eff}, as introduced in our previous work.[11] Δ_{eff} denotes the total signal decay at the experimental DEER evolution time (see the Supporting Information) and is an approximate measure of the average interspin distance for broad $P(R)$ distributions.[11] For increasing interspin mean distance R between two labeling sites Δ_{eff} typically decreases. The lower distance boundary of this method is 1–1.6 nm in aqueous solutions and the assumption of decreasing Δ_{eff} with increasing mean distance of $P(R)$ is only valid for double mutants showing very broad conformational ensembles and, hence, for broad distance distributions, $P(R)$.[11] Thus, our approach is appropriate primarily for the analysis of large, extended proteins like OPN. (Note that PREs are complementary to DEER in terms of length scales. PREs are effective below 2–3 nm only for the present system. Thus, also significant changes in Δ_{eff} do not need to correlate with changes in PREs or differential PRE values.) Furthermore, experimental DEER background functions are necessary for proper data treatment. It should be noted that for folded proteins where one frequently observes strong modulations in DEER time traces a Δ_{eff} analysis would not be possible. In Figure 2 Δ_{eff} values for the six double mutants in the apo and heparin-bound state are shown (the EPR raw data are shown in the Supporting Information Figures S2 and S3). In all cases the binding of heparin leads to a clear decrease in Δ_{eff} indicating increased distances between the labeling sites of the six double mutants. This is in excellent agreement with the expansion of OPN upon heparin binding, observed by means of NMR analysis and also supports an unfolding-upon-binding event.

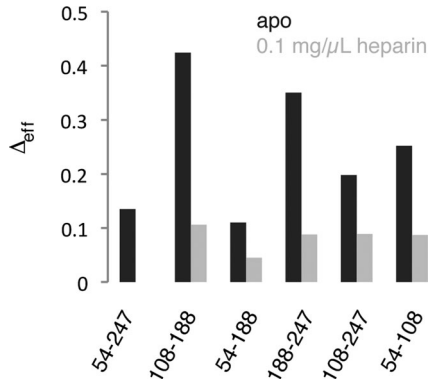

Figure 2. Δ_{eff} values for the six OPN double mutants in the apo (black) and heparin-bound (gray) state. (Δ_{eff} for mutant 54-247 with heparin is 0.)

The observed, "on average" conformational expansion of the central region of OPN upon heparin binding can be rationalized when one takes into account that heparin is a highly negatively charged polyelectrolyte that interacts predominantly electrostatically with its environment. In Figure 3 a the charge distribution map of OPN is shown which highlights patches of low and high charge densities. Heparin has been shown to bind to the positively charged patch of OPN around residues 155, thereby exploiting favorable electrostatic interactions.[8f,11] Yet, the large negatively charged patch around residues 80–120 is likely to experience electrostatic repulsion from heparin and is, therefore, displaced from the central region of OPN around residue 155 upon heparin binding. This leads to the observed expansion of the central region and to positive ΔPRE values as shown in Figure 1 a. In contrast, in the apo state the negatively charged region around C108 is known to be attracted by the positive patch around residue 155, compacting the OPN core.[11] Thus, the OPN–heparin complex reveals an electrostatic binding mode largely governed by complementary charge patterns as often found in molecular recognition processes.[12] To further corroborate these findings we measured the changes in NMR chemical shifts, PRE data (see Figure S6 in the Supporting Information), and DOSY data caused by different salt conditions. The observed changes of NMR parameters and hydrodynamic radius R_H under high salt conditions clearly indicate that the OPN–heparin complex dissociates through NaCl influence (R_H OPN: 3.6 nm; OPN–heparin: 5.2 nm, and OPN–heparin/400 mM NaCl: 3.4 nm).

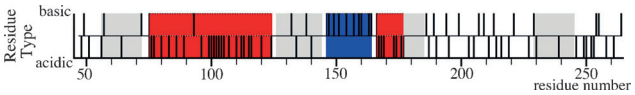

Figure 3. Charge distribution map of OPN. Gray indicates charge-neutral patches, red indicates acidic (negatively charged under experimental pH) residues, and blue basic (positively charged) residues.

The binding of heparin to OPN was also studied by isothermal titration calorimetry (ITC) measurements. From ITC measurements ΔH and ΔS values of -16.3 kcal mol^{-1} and -35 cal mol^{-1} K^{-1} can be obtained for the heparin–OPN binding event assuming an average molecular weight of 17.5 kDa for heparin. These quite large ΔH and ΔS values nearly cancel each other at 293 K with respect to the Gibbs energy of binding ($\Delta G = \Delta H - T\Delta S$). The dissociation constant was determined to 34 μM (see the Supporting Information). Additionally, ITC measurements at different temperatures revealed a positive differential heat capacity, ΔC_p, (about 40 cal mol^{-1} K^{-1}) for heparin binding which further supports the notion that the bound state exhibits more conformational flexibility than the free state. Again, ITC data obtained at 400 mM NaCl confirmed the inhibition of the complex formation under high salt conditions (see Figure S7 in the Supporting Information).

In conclusion we could show, by applying NMR and EPR measurements, that heparin binding leads to an expansion of

the central regions of OPN. Therefore, the interaction mode of this IDP with its ligand can be described as formation of a fuzzy complex (i.e., residual conformational flexibility in the bound state). Although there is local rigidification in the heparin binding cleft (region around residue 155) the resulting conformational entropy penalty is reduced by a compensatory increase in conformational flexibility of the negatively charged region 90–120. The local (or segmental) unfolding and expansion of the OPN core segment thereby significantly contributes to the overall thermodynamic equilibrium balanced between counteracting contributions like solvation enthalpy androtational and translational degrees of freedom and conformational entropy, as is typical for IDPs.[6,14]

We deduce that heparin binding to OPN is predominantly mediated by electrostatic interactions across the interface displaying complementary charge distributions. Given its similar chemical composition, an analogous binding mode can be anticipated for the naturally occurring OPN ligand heparan sulfate. Further, the thermodynamic (entropic) compensation, as measured by NMR and ITC, gained through the structural rearrangements of OPN might be central to the common IDP property of rapid substrate binding and release and the versatility of their host–guest interactions. It is thus instructive to compare our findings with those of a recent study describing the binding of Sic1 to Cdc4 for which a similar binding mode was observed.[15] In this study conformational averaging of Sic1 in the bound state was shown to be relevant for polyvalent interactions that lead to ultrasensitivity and nonlinear binding in response to, for example, phosphorylation. Although the details of binding differ (OPN–heparin: bulk electrostatic patches versus Sic1–Cdc4: polyvalent interactions) entropic compensatory events seem to be present in both systems (OPN–heparin: conformational expansion; Sic1–Cdc4: enhanced conformational entropy through polyvalent interaction) hinting towards a more common phenomenon in the realm of IDPs.

IDPs mediate protein interactions in dynamic networks; for fast and efficient response to external stimuli low energy barriers and facilitated interconversions between different substates are required. This is facilitated by binding modes governed by electrostatics since they allow for considerable conformational plasticity (also through high hydrophilicity),[16] modulating the lifetime and rates of conversions of individual bound states in encounter complex ensembles. We thus anticipate that complementary structural and dynamical adaptations similar to the described OPN–heparin interaction will be observed for intrinsically disordered protein hubs in cellular interaction networks.

Received: September 25, 2013
Revised: November 11, 2013
Published online: March 6, 2014

Keywords: compensatory entropy · intrinsically disordered proteins · NMR spectroscopy · osteopontin · protein complexes

[1] a) P. Tompa, *Trends Biochem. Sci.* **2002**, *27*, 527–533; b) J. Dyson, P. E. Wright, *Nat. Rev.* **2005**, *6*, 197–208.
[2] D. D. Boehr, R. Nussinov, P. E. Wright, *Nat. Chem. Biol.* **2009**, *5*, 789–796.
[3] a) P. R. L. Markwick, T. Malliavin, M. Nilges, *Plos Comput. Biol.* **2008**, *4*, e1000168; b) G. T. Montelione, D. Y. Zheng, Y. P. J. Huang, K. C. Gunsalus, T. Szyperski, *Nat. Struct. Biol.* **2000**, *7*, 982–985; c) V. Ozenne, R. Schneider, M. Yao, J.-r. Huang, L. Salmon, M. Zweckstetter, M. R. Jensen, M. Blackledge, *J. Am. Chem. Soc.* **2012**, *134*, 15138–15148.
[4] H. J. Dyson, P. E. Wright, *Curr. Opin. Struct. Biol.* **2002**, *12*, 54–60.
[5] P. Tompa, M. Fuxreiter, *Trends Biochem. Sci.* **2008**, *33*, 2–8.
[6] V. N. Uversky, *Int. J. Biochem. Cell Biol.* **2011**, *43*, 1090–1103.
[7] a) T. Mittag, J. Marsh, A. Grishaev, S. Orlicky, H. Lin, F. Sicheri, M. Tyers, J. D. Forman-kay, *Structure* **2010**, *18*, 494–506; b) R. Konrat, *Structure* **2010**, *18*, 416–419.
[8] a) G. M. Clore, C. Tang, J. Iwahara, *Curr. Opin. Struct. Biol.* **2007**, *17*, 603–616; b) G. Jeschke, Y. Polyhach, *Phys. Chem. Chem. Phys.* **2007**, *9*, 1895–1910; c) J. Iwahara, C. D. Schwieters, G. M. Clore, *J. Am. Chem. Soc.* **2004**, *126*, 5879–5896; d) M. Drescher, *Top. Curr. Chem.* **2012**, *321*, 91–120; e) T. Bund, J. M. Boggs, G. Harauz, N. Hellmann, D. Hinderberger, *Biophys. J.* **2010**, *99*, 3020–3028; f) G. Platzer, A. Schedbauer, A. Chemeli, P. Ozdowy, N. Coudevylle, R. Auer, G. Kontaxis, M. Hartl, A. J. Miles, B. A. Wallace, O. Glaser, K. Bister, R. Konrat, *Biochemistry* **2011**, *50*, 6113–6124.
[9] a) A. Bellahcène, V. Castronovo, K. U. E. Ogbureke, L. W. Fisher, N. S. Fedarko, *Nat. Rev.* **2008**, *8*, 212–226; b) H. Ponta, L. Sherman, P. A. Herrlich, *Nat. Rev.* **2003**, *4*, 33–45; c) M. Jones, L. Tussey, N. Athanasou, D. G. Jackson, *J. Biol. Chem.* **2000**, *275*, 7964–7974; d) J. L. de Paz, E. A. Moseman, C. Noti, L. Polito, U. H. von Andrian, P. H. Seeberger, *ACS Chem. Biol.* **2007**, *2*, 735–744.
[10] a) W. Hubbell, D. Cafiso, C. Altenbach, *Nat. Struct. Biol.* **2000**, *7*, 735–739; b) W. Hubbell, H. Mchaourab, C. Altenbach, M. Lietzow, *Structure* **1996**, *4*, 779–783.
[11] D. Kurzbach, G. Platzer, M. Henen, T. Schwarz, R. Konrat, D. Hinderberger, *Biochemistry* **2013**, *52*, 5167–5175.
[12] a) B. Honig, A. Nicholls, *Science* **1995**, *268*, 1144–1149; b) N. Sinha, S. J. Smith-Gill, *Curr. Protein Pept. Sci.* **2002**, *3*, 601–614.
[13] D. Hinderberger, H. W. Spiess, G. Jeschke, *Appl. Magn. Reson.* **2010**, *37*, 657–683.
[14] K. K. Frederick, M. S. Marlow, K. G. Valentine, A. J. Wand, *Nature* **2007**, *448*, 325–U323.
[15] a) M. Borg, T. Mittag, T. Pawson, M. Tyers, J. D. Forman-Kay, H. S. Chan, *Proc. Natl. Acad. Sci. USA* **2007**, *104*, 9650–9655; b) T. Mittag, S. Orlicky, W. Y. Choyc, X. Tang, H. Lin, F. Sicheri, L. E. Kay, M. Tyers, J. D. Forman-Kay, *Proc. Natl. Acad. Sci. USA* **2008**, *105*, 17772–17777.
[16] D. Kurzbach, W. Hassouneh, J. R. McDaniel, E. A. Jaumann, A. Chilkoti, D. Hinderberger, *J. Am. Chem. Soc.* **2013**, *135*, 11299–11308.

